SUPPLEMENTARY MATERIALS for Han et al.,
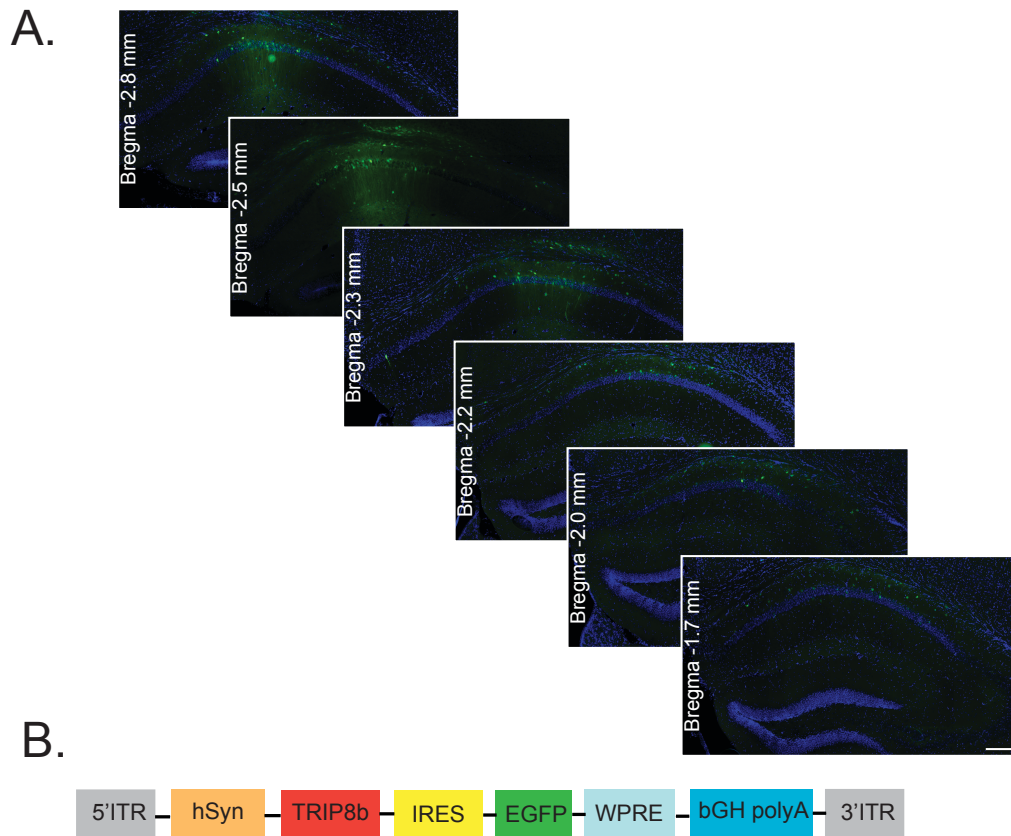## "HCN channel dendritic targeting requires bipartite interaction with TRIP8b and regulates antidepressant-like behavioral effects"

1. SUPPLEMENTARY FIGURES and FIGURE LEGENDS

A.

B.

5'ITR — hSyn — TRIP8b — IRES — EGFP — WPRE — bGH polyA — 3'ITR

Supplementary Figure S1. **(A)**Representative GFP immunostaining illustrates the distribution of AAV-TRIP8b in the dorsal hippocampus four weeks after injection. (Related to Figure 1). AAV-TRIP8b covers the CA1 region with dominant expression mediolaterally (0.5-1mm) and anteroposteriorly (1-1.2 mm). Scale bar represents 200 μm. **(B)** Schematic of AAV-TRIP8b constructs. The expression of TRIP8b was driven by human synapsin (hSyn) promoter and enhanced by woodchuck hepatitis virus post-transcriptional regulatory element (WPRE). ITR, inverted terminal repeat; IRES, internal ribosome entry site; bGH polyA, bovine growth hormone polyadenylation.
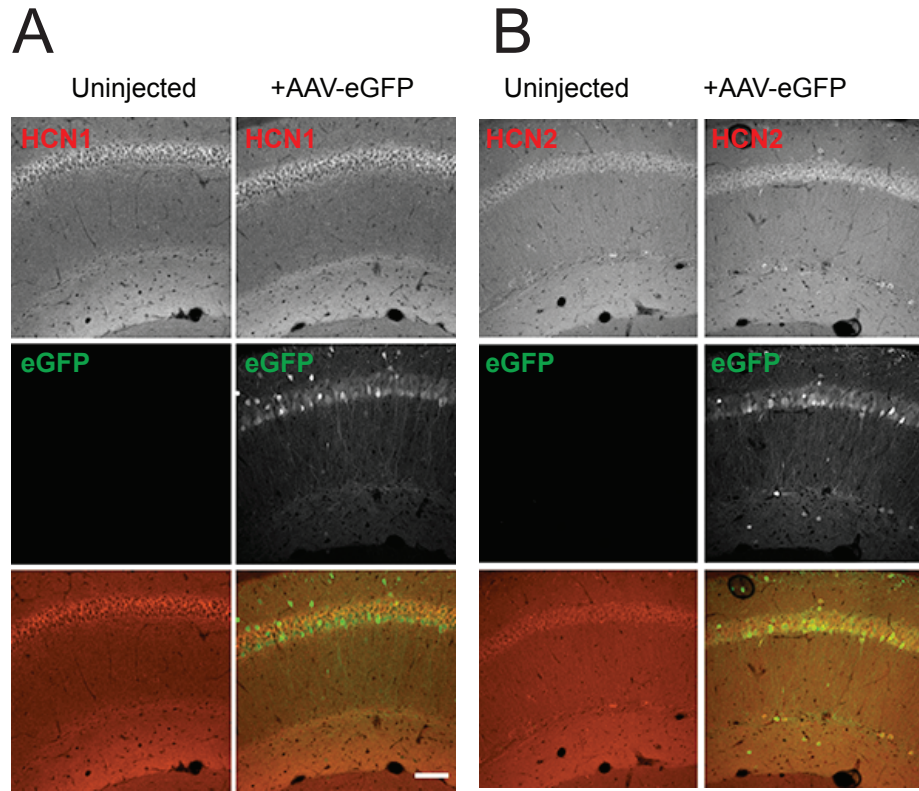
Supplementary Figure S2. **AAV-eGFP fails to rescue distal dendritic targeting of either HCN1 or HCN2 in TRIP8b KO mice.** (Related to Figure 2)
The hippocampi of TRIP8b KO mice were unilaterally injected with AAV-eGFP to examine effects on dendritic targeting of HCN1 (**A**) and HCN2 (**B**). Left hand panels show uninjected (control) hemisphere and right hand panels show the injected hemisphere. Top panels are stained for HCN1 or HCN2 (red), middle panels for eGFP (green), and the lower panels are a composite image of the two. Note that the injected hemisphere shows no difference in HCN1 or HCN2 staining in the SLM relative to the uninjected hemisphere.   Scale bar represents 100 μm.
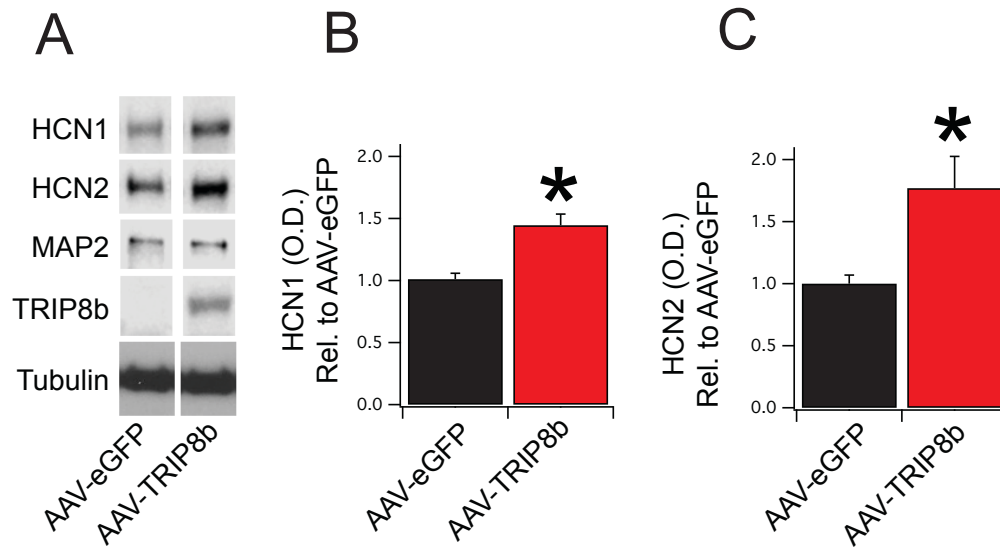
Supplementary Figure S3. **AAV-TRIP8b increases HCN1 and HCN2 total protein expression in the hippocampi of TRIP8b KO mice.** (Related to Figure 2).
A.) Representative immunoblot from hippocampal lysate of TRIP8b KO mice bilaterally injected with AAV-eGFP or AAV-TRIP8b. To ensure that the changes we observed for HCN1 and HCN2 were not the result of neuronal cell death, we also blotted for MAP2 but did not see any differences between the different AAV constructs. All bands appeared near their predicted molecular weights. **B.)** Densitometry analysis for HCN1. Two tail T test indicated a significant difference between AAV-eGFP (1.01±0.04, n=12) and AAV-TRIP8b(1.44±0.08, n=6, t=4.7, p<0.001). **C.)** Densitometry analysis for HCN2. Two tail T test demonstrated a difference between AAV-eGFP (1.00±0.06, n=6) and AAV-TRIP8b (1.76±0.25, n=3, t=3.93, p<0.01). All error bars represent ± s.e.m. and are described above as mean ± s.e.m.
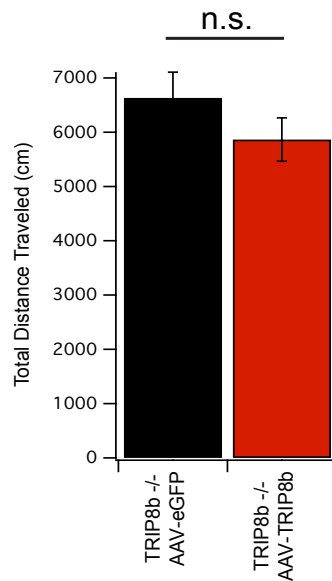
Supplementary Figure S4. **Open field test reveals no difference between bilateral injection of AAV-TRIP8b and AAV-eGFP.** (Related to Figure 2). TRIP8b KO mice were bilaterally injected with either AAV-TRIP8b or AAV-eGFP. After 4 weeks, an open field test was performed to determine if there were any differences in locomotor activity. Mice injected with AAV-eGFP (6632±473cm, n=6) showed no difference in total distance traveled relative to mice injected with AAV-TRIP8b (5864±399cm, n=6) by two tailed T test (p>0.05). Data reported and displayed as mean±s.e.m.
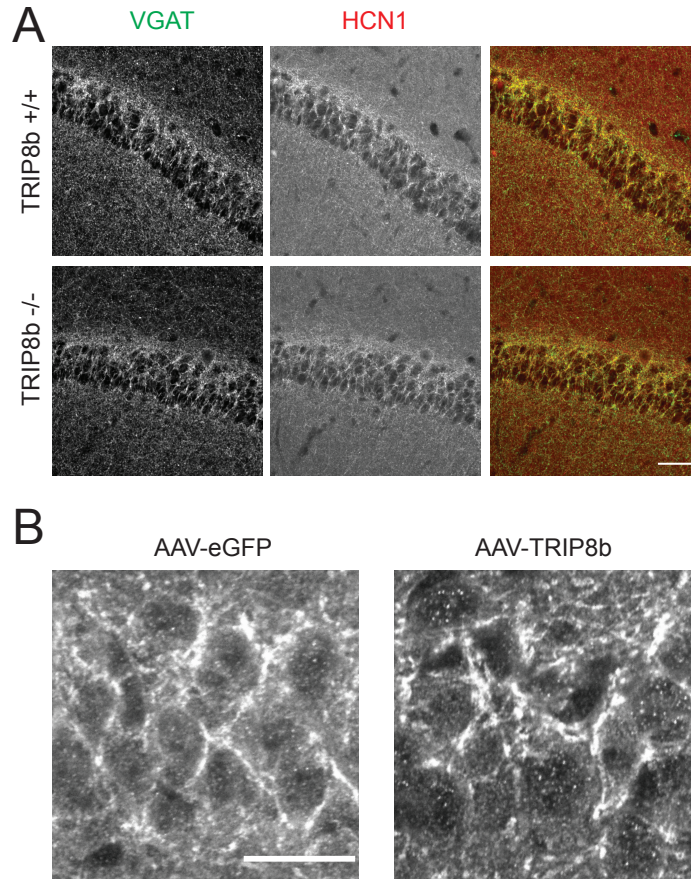
Supplementary Figure S5. **Presynaptic inhibitory terminals in CA1 express HCN1 in a TRIP8b independent manner.** (Related to Figure 2)

(A) Wild Type and TRIP8b KO mice were processed for immunohistochemistry and stained for vesicular GABA transporter (VGAT), an inhibitory presynaptic terminal marker, and HCN1. Note the substantial colocalization of HCN1 at presynaptic terminals in both wild type and TRIP8b KO animals, indicating that loss of TRIP8b does not affect presynaptic HCN1 trafficking. Scale bar represents 40µm. **(B)** TRIP8b KO mice were unilaterally injected with either AAV-eGFP or AAV-TRIP8b and stained for HCN1. In the CA1 cell body layer, we noted no difference in the distribution of HCN1 staining after injection with either AAV-eGFP or AAV-TRIP8b. Scale bar represents 20µm.
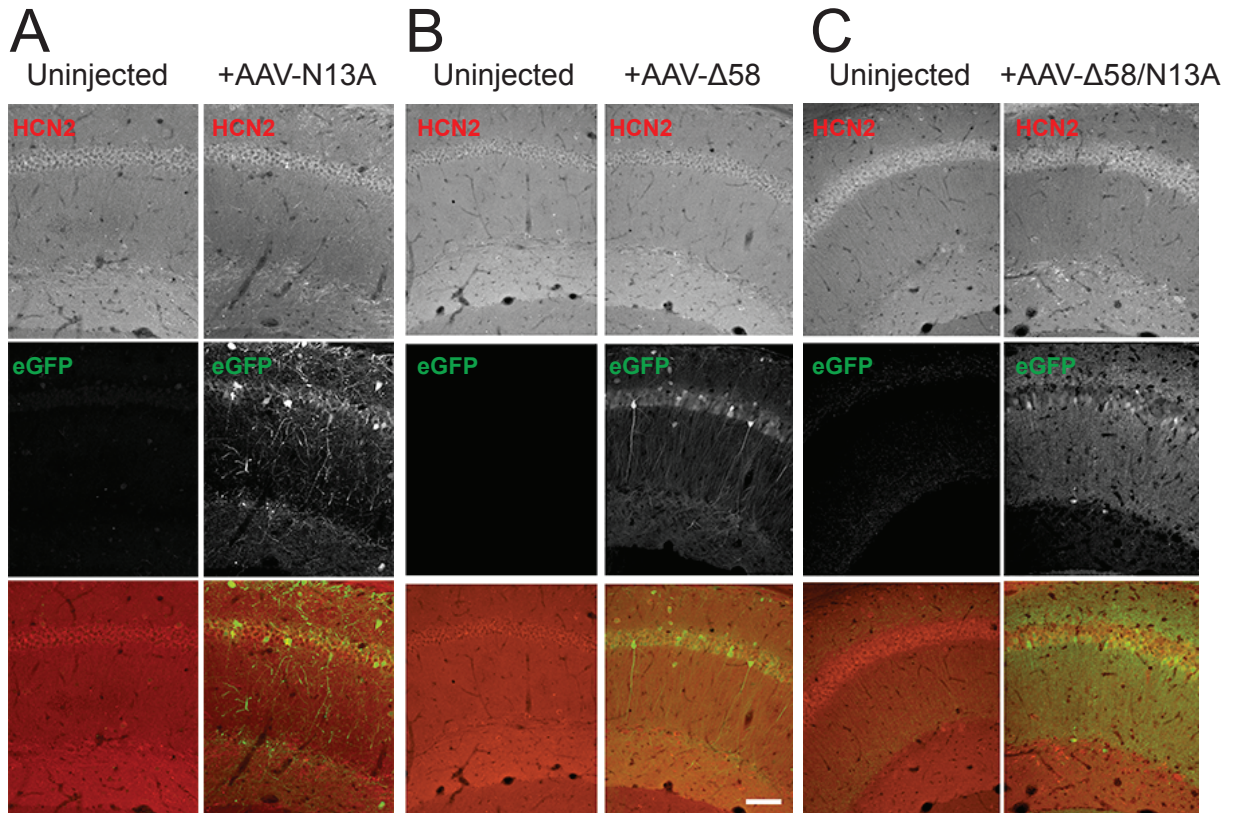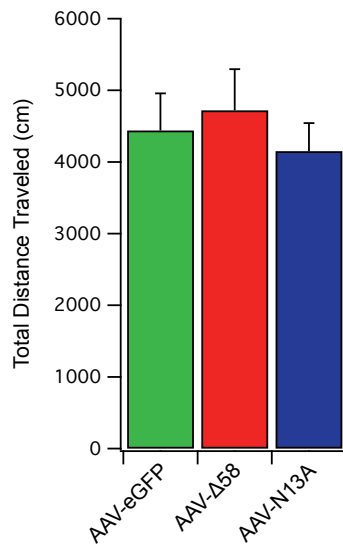
Supplementary Figure S6. **AAV-N13A, AAV-Δ58, and AAV-Δ58/N13A fail to rescue dendritic targeting of HCN2 in TRIP8b KO mice.** (Related to Figure 4)
TRIP8b KO mice were unilaterally injected with AAV-N13A **(A),** AAV-Δ58 **(B),** or AAV-Δ58/N13A **(C).** Display of images is identical to that in **Figure 4.** Scale bar represents 100μm.
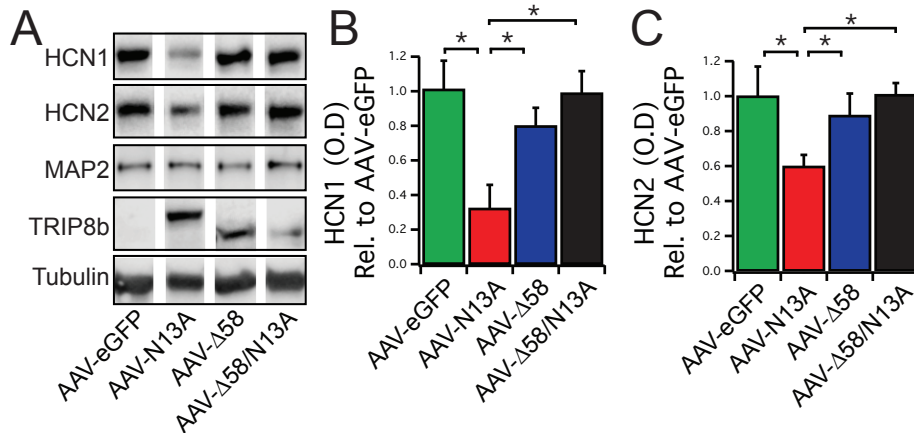
Supplementary Figure S7. **AAV-N13A reduces HCN1 and HCN2 protein expression in the hippocampi of TRIP8b KO mice.** (Related to Figure 4)

A.) Representative immunoblot from hippocampal lysate of TRIP8b KO mice bilaterally injected with AAV-eGFP, AAV-N13A, AAV-Δ58, or AAV-Δ58/N13A. Western blot bands appeared near their predicted molecular weights. Note that the Δ58 TRIP8b mutants are lighter than mutant harboring only the N13A mutation, consistent with the loss of 58 amino acids. **B.)** Densitometry analysis for HCN1. A one way ANOVA examining condition (AAV-eGFP, AAV-N13A, AAV-Δ58, AAV-Δ58/N13A) was significant ($F_{(3,22)}=34.2748$, $p<0.05$) with Tukey's test showing differences between AAV-eGFP and AAV-N13A ($p<0.05$), AAV-N13A and AAV-Δ58($p<0.05$), and AAV-Δ58 and AAV-Δ58/N13A ($p<0.05$). n=12 AAVeGFP, n=7 AAV-N13A, n=4 AAV-Δ58, n=3 AAV-Δ58/N13A. **C.)** Densitometry analysis for HCN2. A one way ANOVA comparing HCN2 was significant ($F_{(3,13)}=9.243$, $p<0.05$) with post-hoc tests showing differences between AAV-eGFP and AAV-N13A ($p<0.05$), AAV-Δ58 and AAV-N13A, and AAV-N13A and AAV-Δ58/N13A ($p<0.05$). n=6 AAV-eGFP, n=4 AAV-N13A, n=4 AAV-Δ58, n=3 AAV-Δ58/N13A. Finally, we observed no changes in MAP2 for the different TRIP8b constructs indicating that the changes in HCN1 and HCN2 were not a consequence of changes in the number of neurons.

<u>Supplementary Figure S8.</u> **Bilateral injection of AAV-eGFP, AAV-N13A, or AAV-Δ58 does not increase locomotor activity on open field test.** (Related to Figure 4)
TRIP8b KO animals were bilaterally injected with AAV-eGFP, AAV-N13A, or AAV-Δ58 (n=5,5,5). One month later the locomotor activity of the mice was assayed by open field testing. Total distance traveled in centimeters was recorded, although no difference between the three conditions was observed by one way ANOVA ($F_{(2,12)}=0.32$, $p>0.5$). Data shown as mean ± s.e.m.

2. SUPPLEMENTARY TABLES

Genotype	Virus	Membrane Resistance, MΩ	Membrane Capacitance, pF	Resting Membrane Potential, mV	Half Activation Potential, mV	Time Constant, ms
TRIP8b KO	AAV-eGFP	226.4 (32.6, 9)	193.5 (27.0, 9)	-67.4 (2.9, 9)	-99.55 (4.3, 7)	250 (28, 7)
TRIP8b KO	AAV-TRIP8b	198.8 (30.3, 8)	176.0 (20.7, 8)	-69.4 (3.8, 8)	-90 (3.5, 7)	186 (14, 7)

Supplementary Table S1. **Summary of membrane properties from CA1 pyramidal neurons infected with AAV-eGFP or AAV-TRIP8b. (Related to Figure 1)**
Table listing the genotype of the animal used for the experiment, the virus injected, and then the membrane resistance and resting membrane potential. Half activation potential was determined from Boltzmann fits of tail-current amplitude recorded at -80 mV after steps from -60 to -140 mV in 10mV increments. The time constant is the result of a monoexponential fit of channel activation when stepping from a holding potential of -60mV to -120mV. Two-tail T tests were not significant for any values (p>0.05 in all cases). Data presented as mean (s.e.m., n).

Genotype	Virus	Membrane Resistance, MΩ	Resting Membrane Potential, mV	Half Activation Potential, mV	Time Constant, ms
TRIP8b KO	AAV-eGFP	376.8 (87.3, 9)	-67.4 (2.9, 9)	-99.55 (4.3, 7)	250 (28, 7)
TRIP8b KO	AAV-N13A	313.7 (61.2, 7)	-68.3 (3.4, 7)	-101.4 (2.0, 7)	269 (55, 7)
TRIP8b KO	AAV- Δ58	254.9 (29.9, 6)	-73.4 (1.3, 6)	-94.62 (4.1, 4)	301 (77, 5)

Supplementary Table S2. **Summary of membrane properties from CA1 pyramidal neurons infected with AAV-N13A or AAV-Δ58 (Related to Figure 3)**
Table displaying the membrane properties of CA1 pyramidal neurons from TRIP8b KO mice infected with AAV-eGFP, AAV-N13A, or AAV-Δ58. Note that the information for the AAV-eGFP condition is identical to that presented in Table S1 but is reproduced here for comparison. A one way ANOVA comparing the three conditions for each parameter was not significant ($p > 0.05$ in all cases). Data presented as Mean (s.e.m., n).

3.Supplementary Experimental Procedures

Viral injections

Generation of global TRIP8b knockout mice used in this study has been previously described[1]. Wild type C57Bl/6 mice were obtained from Jackson Laboratories. Male mice (age 4-6 weeks) were anesthetized with an intraperitoneal injection of ketamine (100 mg/kg) and xylazine (10 mg/kg) and mounted on a stereotaxic instrument (Stoelting, Wood Dale, IL). A small incision was made to expose the skull and a small craniotomy made with a dental drill. 1µl of 3 x 10^{12} vector genome (vg)/ ml of AAV was injected into the dorsal hippocampus of TRIP8b KO mice at a rate of 0.3 µl/min via a 5 µl Hamilton syringe. The injection co-ordinates were 2.3 mm A/P, ±1.3 mm M/L, -1.7 mm D/V. The needle was slowly removed at a rate of 1 mm min^{-1} following holding in the injection site for 5min to allow for diffusion of the virus.

Behavioral tests

Animal numbers required to observe differences in behavioral tests (TST, FST, OFT) were estimated based on experiments previously performed in our lab[1]. Prior to testing, all mice were group housed 3-5 per cage and provided water and rodent chow *ad libitum*. For experiments using TRIP8b-KO mice, appropriate TRIP8b-KO wildtype mice were used as controls with their corresponding homozygous KO counterparts. All mice tested were males between 8-12 weeks old at the time of behavioral testing. Immediately prior to behavioral testing, all mice acclimated to the testing room in their home cages for at least 30 minutes, and all tests were performed during the light phase of a 12hr dark/light cycle. The testing room was sound-proofed, and between each trial of testing, all apparatuses or arenas were cleaned with 70% ethanol. The experimenter was blinded to the genotypes and treatment status of the mice to prevent bias, and the subjects were randomized before testing. All animals that survived surgery and post-operative recovery were included for analysis, with exceptions made for animals that were euthanized on the recommendation of a veterinarian.

The Open Field Test was administered as previously described[1]. Briefly, mice were placed into the center of an open arena (56cm x 56cm) that was moderately lit with white light, and their XY movements were tracked and recorded for 10 minutes with overhead cameras and video tracking software (LimeLight 3). Total locomotion, time spent in the center of the arena, and time spent in the periphery were analyzed.

We tested the mice on the Tail Suspension and Forced Swim Tests to assess antidepressant-like behavior, as previously described[1]. For the Tail Suspension Test, we suspended the mice by their tails for 6 minutes and measured the amount of time they spent without struggling, noted as immobility time. Struggling for this assay is defined as moving their fore or hind limbs. Next for the Forced Swim Test, we placed the mice in 24°C +/- 1°C tap water for 6 minutes. After 2 minutes had passed, we measured the amount of time spent immobile for the remaining 4 minutes. Immobility was defined as cessation of purposeful movement, except for small twitches necessary to keep the mouse upright. The dirty water was emptied after each trial and replaced with clean tap water.

Plasmid constructs.
All restriction enzymes were purchased from New England Biolabs (NEB). All oligonucleotides for use in PCR amplification and oligo insertion were synthesized by Integrated DNA Technologies (IDT). All plasmids were verified by DNA sequencing (Northwestern Sequencing

Core).

AAV constructs.

The DNA plasmid for *pAAV-hsynapsin-Cre-IRES-eGFP* was kindly provided by Dr. Pavel Osten (Cold Spring Harbor Laboratory). *pAAV-hsynapsin-IRES-eGFP* was generated by excising *Cre* using *EcoRI* followed by insertion of restriction sites with oligonucleotides (For- AAT TCA AGC TGG ATA TCG GGC and Rev- AAT TGC CCG ATA TCC AGC TTG). *pAAV-hsynapsin-TRIP8b -IRES-eGFP* (*pAAV-TRIP8b*) was generated by *EcoRI/XbaI* digestion of *pXEGFP-TRIP8b(1a-4)* [2] followed by blunt ligation and insertion into *pAAV-hsynapsin-IRES-eGFP*, which was digested by *EcoRV*. *pAAV-N13A* was generated by *EcoRV/Bsu361* digestion of *pXEGFP-TRIP8b(1a-4)(TPR3-N13A)* followed by subcloning into *pAAV-1a-4* at *EcoRV/Bsu361* sites. *pAAV-Δ58* was generated by *SpeI/BamHI* digestion of pXEGFP-TRIP8b (1a-4)(Δ58) followed by subcloning into *pAAV-1a-4* at *SpeI/BamI* sites[3]. AAV serotype 2/8 vectors were produced by the Gene Therapy Program of the University of Pennsylvania.

Immunohistochemistry.
Mice were deeply anesthetized with isoflurane and transcardially perfused with cold PBS followed by 4% paraformaldehyde. Brains were then removed and post-fixed in 4% PFA overnight. 30 μm coronal sections were made on a vibratome (Leica, Buffalo Grove, IL). Antigen retrieval was performed with 10 mM Na-citrate, pH 9.0, for 10 minutes at 80ºC prior to blocking in PBS with 5% normal goat serum and 0.03% Triton X-100 for 1 hour. Primary antibodies were diluted in blocking solution and applied overnight at 4ºC. Sections were washed 3 times prior to a 1 hour incubation at room temperature in secondary antibody, followed by 3 additional washes in PBS. DAPI was included in the final wash and tissue was then mounted on glass slides with PermaFluor (Thermo Fisher Scientific, Fremont, CA). Imaging was performed at the Northwestern University Center for Advanced Microscopy on a Nikon A1R confocal microscope using NIS Elements software (Nikon, Melville, NJ) and TissueGnostics, and analyzed using FIJI. Primary antibodies used were custom guinea pig anti-HCN1, guinea pig anti-HCN2, and rabbit anti-TRIP8b[2], and rabbit anti-GFP (Millipore, Temecular, CA). The sensitivity and specificity of these antibodies have been verified extensively in previous reports[4-6]. All secondary antibodies were purchased from Invitrogen. For quantification of images (Figures 2 and 4), custom written routines in MATLAB (Mathworks, Natick, MA) were used. Regions of interest (ROI) were drawn over the stratum oriens and stratum pyramidale. A large ROI was also drawn over the region encompassing the stratum radiatum and stratum lacunosum moleculare and then subdivided into ten equally spaced ROIs. The mean intensity of the staining within each ROI was then used for subsequent downstream analyses. Within each slice, the staining intensity of the injected hemisphere was divided by the intensity of the staining in the corresponding ROI from the contralateral hemisphere.

Western blotting.
Western blotting was performed as previously described[2]. Primary antibodies used were: custom rabbit anti-HCN1, rabbit anti-HCN2 and guinea pig anti-TRIP8b[2], rabbit anti-MAP2 (Millipore Temecular, CA); and mouse anti-tubulin (Millipore Temecular, CA). Primary antibodies were diluted in blocking solution containing 5% milk and 0.1% Tween-20 in TBS (TBS-T). Band intensities were quantified using NIH ImageJ software and normalized to the anti-tubulin signal for each sample.

Electrophysiology

Mice were deeply anesthetized with isoflurane, decapitated, and the whole brain was rapidly dissected into ice-cold sucrose solution containing (in mM): 190 sucrose, 10 NaCl, 2.5 KCl, 25 NaHCO$_3$, 1.25 NaH$_2$PO$_4$, 0.5 CaCl$_2$, 7 MgCl$_2$, 25 dextrose; pH 7.4. All solutions were continuously bubbled with 95% O$_2$/5% CO$_2$. 300 μm sagittal slices were made using a vibratome (Leica) and immediately transferred to a 35ºC holding chamber containing ACSF (125 NaCl, 2.5 KCl, 25 NaHCO$_3$, 1.25 NaH$_2$PO$_4$, 2 CaCl$_2$, 1 MgCl$_2$, 25 dextrose; pH 7.4). After a 25-minute incubation period, the chamber was allowed to equilibrate to room temperature for ≥30 minutes before use. For recording, slices were transferred to a custom chamber perfused with room temperature (22±1ºC), oxygenated ACSF at 1-2 mL/min. Electrodes (4-6 MΩ) were pulled on a Sutter P87 pipette puller and filled with intracellular solution containing: 115 K-gluconate, 20 KCl, 10 HEPES, 10 Na-phosphocreatine, 2 Mg-ATP, 0.3 Na-GTP, 0.2% biocytin. KOH was added to pH 7.3. Whole-cell recordings were made with a PC-ONE amplifier (Dagan), filtered at 3 kHz, and digitized at 20 kHz using an InstruTECH ITC16. A calculated liquid junction potential of 13 mV was compensated prior to approaching each cell. Series resistance was monitored throughout each experiment, and cells were discarded if the series resistance exceeded 30 MΩ. Data acquisition and analysis was performed in IgorPro 6 (WaveMetrics) using custom macros. Membrane resistance was derived from the slope of the regression line for voltage responses to small-amplitude current injections. Monoexponential fits of the first 200 ms of these traces were used to obtain the membrane time constant, from which membrance capacitance was estimated by dividing by the membrane resistance. I$_h$ amplitude at -120 mV was obtained by subtracting the instantaneous current after the capacitive transient from the steady-state current at the end of a 2 s step. Half-activation voltage was determined from Boltzmann fits of tail-current amplitudes recorded at -80 mV after steps from -60 to -140 mV in 10mV increments. Time constants of I$_h$ activation were derived from a monoexponential fit of steps from a holding potential of -60mV to -120mV.

4. Supplemental References

1. Lewis AS, Vaidya SP, Blaiss CA, Liu Z, Stoub TR, Brager DH *et al.* Deletion of the hyperpolarization-activated cyclic nucleotide-gated channel auxiliary subunit TRIP8b impairs hippocampal Ih localization and function and promotes antidepressant behavior in mice. *J Neurosci* 2011; **31**: 7424–7440.

2. Lewis AS, Schwartz E, Chan CS, Noam Y, Shin M, Wadman WJ *et al.* Alternatively spliced isoforms of TRIP8b differentially control h channel trafficking and function. *J Neurosci* 2009; **29**: 6250–6265.

3. Han Y, Noam Y, Lewis AS, Gallagher JJ, Wadman WJ, Baram TZ *et al.* Trafficking and gating of hyperpolarization-activated cyclic nucleotide-gated channels are regulated by interaction with tetratricopeptide repeat-containing Rab8b-interacting protein (TRIP8b) and cyclic AMP at distinct sites. *J Biol Chem* 2011; **286**: 20823–20834.

4. Shin M, Simkin D, Suyeoka GM, Chetkovich DM. Evaluation of HCN2 abnormalities as a cause of juvenile audiogenic seizures in Black Swiss mice. *Brain Res* 2006; **1083**: 14–20.

5. Shin M, Chetkovich DM. Activity-dependent regulation of h channel distribution in hippocampal CA1 pyramidal neurons. *J Biol Chem* 2007; **282**: 33168–33180.

6. Chung WK, Shin M, Jaramillo TC, Leibel RL, LeDuc CA, Fischer SG *et al.* Absence epilepsy in apathetic, a spontaneous mutant mouse lacking the h channel subunit, HCN2. *Neurobiol Dis* 2009; **33**: 499–508.